JOURNAL OF THERMOPHYSICS AND HEAT TRANSFER
Vol. 14, No. 3, July–September 2000

Nonequilibrium Planar Interface Model for Solidification of Semitransparent Radiating Materials

Chengcai Yao,* G.-X. Wang,† and B. T. F. Chung‡
University of Akron, Akron, Ohio 44325-3903

A nonequilibrium solidification model for semitransparent materials is presented. Consideration is given to a planar layer of emitting, absorbing, and scattering medium subject to radiative and convective cooling. The enthalpy method is used to formulate the phase-change problem together with radiative transfer equation taking into account internal emitting, absorbing, and scattering. A planar interface nonequilibrium solidification is assumed with crystalline phase nucleated on the surface at a given nucleation temperature, which may be significantly lower than the equilibrium melting temperature of the material. A linear kinetics relationship is introduced to correlate the unknown solidification temperature to the interface velocity. A fully implicit finite volume scheme is used to solve the problem with the solidification interface tracked by a modified interface tracking method. The radiative transfer equation is solved using the discrete ordinates method. Internal radiation enhances the latent heat removal and thus leads to a higher interface velocity and a larger melt undercooling. Optical thickness and the conduction-radiation parameter are two important parameters that affect the solidification process. In the presence of external convective cooling, effect of internal radiation is small in the early stage of solidification.

Nomenclature

c = specific heat, J/kg K
D = thickness of the layer, m
H = dimensionless enthalpy, $(h\text{-}cT_m)/cT_m$
H_R = convection-radiation parameter, $h_c/(\sigma T_m^3)$
h = enthalpy, J/kg
h_c = convective heat-transfer coefficient, W/m^2 K
I = intensity of radiation, W/m^2 sr
$\bar{I}$ = normalized intensity of radiation, $I/(4\sigma T_m^4)$
k = thermal conductivity, W/m K
N = conduction-radiation parameter, $k/(4\sigma T_m^3 D)$
n = refractive index
q_r = radiative heat flux, W/m^2
$\bar{q}_r$ = dimensionless radiative heat flux, $q_r/(4\sigma T_m^4)$
S = dimensionless interface position, s/D
St = Stefan number, cT_m/λ
s = interface position, m
T = absolute temperature, K
T_e = temperature of the environment, K
T_m = equilibrium freezing temperature, K
T_N = nucleation temperature, K
T_s = interface temperature, K
T_0 = initial temperature, K
t = time, s
V_s = dimensionless interface velocity, $\mathrm{d}S/\mathrm{d}\tau$
X = dimensionless coordinate, x/D
x = coordinate in the direction across the slab, m
β = extinction coefficient of the medium, m^{-1}
θ = dimensionless temperature, T/T_m
θ_e = dimensionless environment temperature, T_e/T_m
θ_s = dimensionless interface temperature, T_s/T_m
κ_D = optical thickness of the layer, βD
λ = latent heat of fusion, J/kg
μ = dimensionless linear kinetics coefficient, $(\rho c \mu_k/4\sigma T_m^2)$
μ_k = linear kinetics coefficient, m/s K
ξ = direction cosine of a radiation ray
ρ = density, kg/m^3
ρ^0, ρ^i = reflectivities to external and internal incidence
σ = Stefan–Boltzmann constant, 5.6705×10^{-8} W/m^2 K^4
τ = dimensionless time, $(4\sigma T_m^3/\rho c D)t$
Ω = solid angle, sr
ω = single scattering albedo

Introduction

THE effect of internal irradiation on melting or solidification has long been realized.[1,2] Habib[3,4] is probably the first who analytically solved the phase-change problem of a semi-infinite semitransparent material by employing a heat-balance integral method.[5] Later, Abrams and Viskanta[6] devised a more rigorous treatment of the melting problem of a semitransparent material in a one-dimensional domain. They found that the internal radiative heat transfer has a significant effect on the phase-change velocity and temperature profiles in both the solid and the liquid domains. Chan and coworkers[7,8] proposed that, under an equilibrium condition, there should exist a two-phase zone between the liquid and the solid phases. They solved the solidification and melting problem in an absorbing–emitting semi-infinite body using this model. Experimental studies were carried out by Diaz and Viskanta[9] and Webb and Viskanta.[10] They investigated the melting process of n-octadecane, a semitransparent phase-change material under the irradiation of a tungsten filament lamp. The measured interface locations and temperature profiles agreed very well with their analyses. Effects of internal radiation on phase change were also investigated by Seki et al.,[11] Cho and Ozisik,[12] Oruma et al.,[13] and Kim and Yimer.[14]

All of these phase-change models of semitransparent materials assume a local equilibrium condition at the solidification front. This assumption is valid only for the situation when the material has a large dimension and heat-transfer rate is relatively small. Some processes such as laser material processing and spray casting are characterized by small material dimensions and high heat-transfer rates; in these cases nonequilibrium kinetics effects of phase change become important, and therefore the local-equilibrium condition is not valid any more.[15] In addition, local undercooling or overheating can be introduced by excessive internal radiative heat transfer in a semitransparent material experiencing phase change,[6] and this phenomenon, strictly speaking, cannot be described by an equilibrium

Received 9 August 1999; presented as Paper 99-150 at the 33rd National Heat Transfer Conference, Albuquerque, NM, 15–17 August 1999; revision received 1 February 2000; accepted for publication 16 March 2000.

*Research Assistant, Department of Mechanical Engineering.
†Assistant Professor, Department of Mechanical Engineering.
‡F. Theodore Harrington Professor, Department of Mechanical Engineering; bchung@uakron.edu.

phase-change model. For nonequilibrium phase-change processes melting or solidification will not take place at the equilibrium melting temperature, and a large melt undercooling or solid overheating can exist at the interface. Nonequilibrium kinetics relationships are therefore needed to provide additional mathematical equations to complete the modeling of the problem.

This paper presents a one-dimensional nonequilibrium solidification model for semitransparent materials with internal radiation. The model deals with a slab of emitting-absorbing-scattering semitransparent material subject to radiative and convective cooling on its surfaces. Both conduction and internal radiation are taken into account. Solidification starts on the surface with a given nucleation temperature below the equilibrium melting temperature of the material. A linear solidification kinetics relationship is introduced to correlate the liquid/solid interface moving velocity and the interface temperature, which are two unknowns and must be determined as part of the solution. The corresponding mathematical problem is solved numerically. The enthalpy method and the fully implicit control volume scheme[16] are used to treat heat conduction and phase change inside the slab, whereas a discrete ordinates method[17] is used to deal with the radiative heat transfer. Because exact tracking of the interface location is essential to determine accurately the interface parameters, a modified interface tracking method of Voller and Cross[18] is used to track the liquid/solid interface during solidification. This interface tracking method is similar to the one developed by Fabbri and Voller[19] for a nonequilibrium solidification in the absence of radiation. Finally, selected results are presented to illustrate the unique features of nonequilibrium solidification of semitransparent materials.

Physical Problem and Mathematical Formulation

Consideration is given to a slab of semitransparent material that is emitting, absorbing, scattering, and heat conducting. The slab has a thickness of D and is initially melted to a high temperature T_0. It is then suddenly exposed to a cold environment so that heat is transferred from the slab by both radiation and convection. For the sake of convenience, heat transfer from both sides of the slab is assumed to be symmetrical; therefore, only a half-thickness of the slab needs to be considered, as shown in Fig. 1. The following assumptions are made to simplify the analysis: 1) the material is gray, 2) all material properties are temperature independent and phase independent, 3) solidification is assumed to take place at a planar solid/liquid interface, and 4) the scattering is isotropic.

Governing Equations

Under the preceding assumptions the governing equation of the system under consideration can be written as follows, using the dimensionless variables defined in the nomenclature:

$$\frac{\partial H}{\partial \tau} = N\frac{\partial^2 \theta}{\partial X^2} - \frac{\partial \bar{q}_r}{\partial X} \tag{1}$$

The temperature and enthalpy are related to each other by

$$\theta = \begin{cases} H + 1 & \text{in the solid region} \\ H + 1 - 1/St & \text{in the liquid region} \end{cases} \tag{2}$$

Equations (1) and (2) form the so-called enthalpy formulation of the phase-change problem.

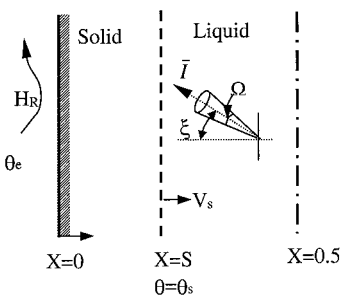

Fig. 1 Schematic of the physical problem and the coordinate system.

The radiation term in Eq. (1) can be found in standard texts (e.g., Refs. 20 and 21):

$$\frac{\partial \bar{q}_r}{\partial X} = \kappa_D(1-\omega)\left(n^2\theta^4 - \int_{4\pi} \bar{I}\,\mathrm{d}\Omega\right) \tag{3}$$

The normalized intensity of radiation $\bar{I}$ is solved from the radiative transfer equation (RTE). The RTE in a one-dimensional form can be written as

$$\frac{\xi}{\kappa_D}\frac{\mathrm{d}\bar{I}}{\mathrm{d}X} = -\bar{I} + (1-\omega)\frac{n^2\theta^4}{4\pi} + \frac{\omega}{4\pi}\int_{4\pi} \bar{I}(X,\Omega)\,\mathrm{d}\Omega \tag{4}$$

Nonequilibrium Solidification with Undercooling

Solidification is assumed to be initiated at the surface of the slab at a prescribed nucleation temperature T_N that is below the equilibrium melting temperature of the material. Because the solidification temperature is an unknown in this case, a nonequilibrium kinetics relationship is needed to complete the mathematical description of the problem. As a first approximation, a linear relationship is used to relate the degree of melt undercooling at the interface to its moving velocity[15]:

$$V_s = \frac{\mathrm{d}S}{\mathrm{d}\tau} = \mu(1-\theta_s) \tag{5}$$

where the dimensionless linear kinetics coefficient μ can be evaluated from the solidification kinetics (e.g., Ref. 22). Equation (5) is an additional condition needed to locate the interface position during solidification. One of the advantages of the enthalpy formulation is that it does not require an explicit track of the solid/liquid interface. In the present situation, however, the solid/liquid interface is continuously tracked during solidification because accurate information about the interface is needed when Eq. (5) is employed.

Boundary and Initial Conditions

At the surface of the slab $X = 0$, the intensity of radiation can be written as[21]

$$\bar{I}(0,\Omega) = \frac{(1-\rho^0)\theta_e^4}{4\pi} + \frac{\rho^i}{\pi}\int_{\xi<0} \bar{I}(0,\Omega')|\xi|\,\mathrm{d}\Omega' \tag{6}$$

The surface is assumed to be diffusive, and the reflectivities ρ^0 and ρ^i are determined by integrated averages from the Fresnel reflection relations.[23] At the symmetry line ($X = 0.5$) the intensity is symmetrical.

Because the radiation passing through or reflected by the boundary has been taken into account in the solution of radiative transfer equation [Eq. (4)], the boundary condition for Eq. (1) only involves external convection and conduction. In the case when the slab is subject to convective cooling, one has

$$4N\frac{\partial \theta}{\partial X} = H_R(\theta - \theta_e) \quad \text{at} \quad X = 0 \tag{7}$$

At the symmetry boundary

$$\frac{\partial \theta}{\partial X} = 0 \quad \text{at} \quad X = 0.5 \tag{8}$$

For convenience, we have assumed that the ambient temperature in Eq. (7) is the same as the environment temperature θ_e. In the limiting case of opaque materials, internal radiation is negligible, and it is conventional to assume that the radiative heat loss emanates from the surface. Equation (7) is then modified as

$$4N\frac{\partial \theta}{\partial X} = H_R(\theta - \theta_e) + (1-\rho^0)\left(\theta^4 - \theta_e^4\right) \quad \text{at} \quad X = 0 \tag{9}$$

where $(1-\rho^0)$ defines the emissivity of the surface.

Initially, the slab is assumed to be in a liquid state at the temperature T_0. Solidification starts when the surface temperature reaches the preset nucleation temperature T_N.

Numerical Solution

The problem is solved using a fully implicit finite volume method. To track the interface accurately and to eliminate the stepwise variation of the predicted interface locations, an interface tracking technique based on the work by Voller and Cross[18] is implemented. Briefly, a variable time step is chosen such that the solidification interface is located at the nodal plane at each time step. The value of the time step, given by $\Delta\tau = \Delta X / V_s$, is a function of the current interface velocity and the grid density and is obtained by iteration. As a result, generally a fine grid has to be used in order to predict the accurate solidification rate and to speed up the calculation at each time step.

The radiative transfer equation is solved using the discrete ordinates (S_N) method. The detailed solution procedure for a combined heat-transfer problem was illustrated elsewhere[24] and will not be repeated here. The S_4 method is found to be sufficient in accuracy.

The iterative solution procedures can be summarized as follows. At the cooling stage of the superheated melt, the implicit solution is performed using a fixed small time step, typically $\Delta\tau = 0.005$. The radiative transfer equation and the energy equation are solved simultaneously and iteratively at each time step. After the onset of solidification, the calculation involves two types of iterations: one for the determination of the time step and the other the typical implicit solution procedure. The solution process at each advancement of time begins with a guessed time step, and then proceeds to solve for the enthalpy and temperature distributions. The interface velocity and thus the time step are then updated using the new interface temperature. In all calculations presented here, a convergence is assumed to be achieved when the relative variation of the temperature is within 10^{-6} at each node and that of the time step is 10^{-3} during two successive iterations.

All solutions are checked against various grid densities. A uniform grid with $\Delta X = 0.0025$ (i.e., 201 nodes) produces the grid-independent results. The differences between the calculated interface locations and the solidification times using $\Delta X = 0.0025$ and those using $\Delta X = 0.00333$ (i.e., 151 nodes) are less than 0.15%.

Results and Discussion

Nonequilibrium solidification of a semitransparent material is a complex process controlled by many parameters. This study only focuses on the effect of internal radiative heat transfer on nonequilibrium solidification characteristics. The parameters of particular interest include the optical thickness κ_D and the conduction-radiation parameter N. The combined effect of internal radiation and external convective cooling is also studied through the convection-radiation parameter H_R. The ranges of these parameters are chosen among those proposed by Siegel.[23] For the results presented here, the scattering albedo is set equal to zero, i.e., $\omega = 0$, the refractive index $n = 1.5$, and the Stefan number $St = 2$ without losing generality. The environment temperature is assumed to be much lower than that of the slab, i.e., $\theta_e \cong 0$. The nucleation temperature is set to be $T_N / T_m = 0.9$ (see, e.g., Refs. 25 and 26). Initially the melt is assumed to be superheated at temperature $T_0 / T_m = 1.05$.

First, a direct check of the numerical methods used in this study is provided by Fig. 2, which depicts an excellent agreement between a limiting solution of the present problem and the exact Neumann solution.[27] The present solution was obtained by assigning very large values to H_R and μ (e.g., H_R and $\mu = 1000$), the same properties of the liquid and solid phases, and setting the radiative heat flux to zero (i.e., $\kappa_D = 0$) in the code. Under these conditions the short time solution should correspond to the solution for a semi-infinite opaque material with the first-kind boundary condition, as demonstrated in Fig. 2.

For the most semitransparent materials with complex crystallographic structures, solidification kinetics is diffusion controlled, and their linear kinetics coefficients are very small.[28] In the following, a small value of μ, i.e., $\mu = 5$ is used for most of the calculations. Choosing a slow kinetics will also emphasize the kinetics effects or the nonequilibrium effects. The results to be presented first are for the case when the radiative cooling is the sole mode of heat transfer from the slab to the environment, i.e., $H_R = 0$. The effect of the convective heat transfer is then introduced next through nonzero values of H_R. Finally, the kinetics effect is discussed.

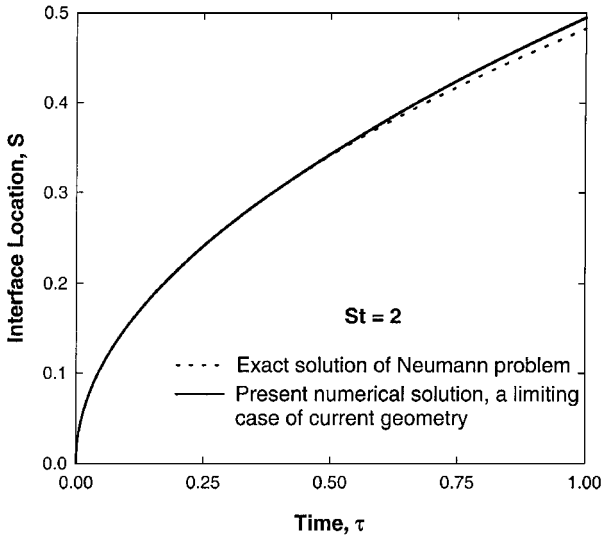

Fig. 2 Comparison of a limiting solution with the exact solution of Neumann problem.

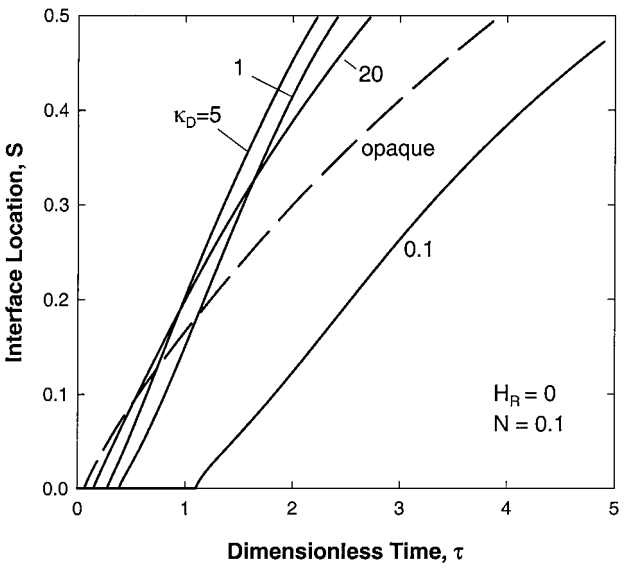

Fig. 3 Interface location as a function of time under pure radiative cooling ($H_R = 0$) for various optical thicknesses with the conduction-radiation parameter $N = 0.1$.

Nonequilibrium Solidification Characteristics of a Semitransparent Material

The characteristics of nonequilibrium solidification of a semitransparent material and the effect of the internal radiation can be best illustrated by the case when the convective cooling is neglected, i.e., when $H_R = 0$. Figure 3 shows the interface location as a function of dimensionless time for the optical thickness $\kappa_D = 0.1$, 1, 5, and 20. The smaller the value of κ_D, the more transparent the material is. The opaque material in Fig. 3 corresponds to an infinite κ_D. A radiation-conduction parameter of $N = 0.1$ is used. Several features can be observed from this figure. First, the solidification rates vary with the optical thicknesses. For example, the total solidification time τ for the opaque material is about 3.9, and it reduces to about 2.7 for $\kappa_D = 20$ and 2.2 for $\kappa_D = 5$. Further reducing κ_D to 1 extends the solidification time to 2.4, however. When $\kappa_D = 0.1$, the solidification rate becomes much slower than that for the opaque material because of the reduced radiation heat transfer between the medium and the environment. This pattern is consistent with the effects of

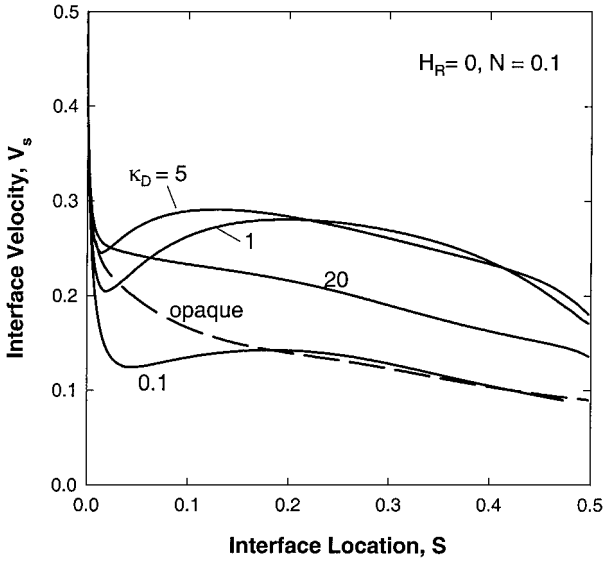

Fig. 4 Interface velocity as a function of the interface location under pure radiative cooling ($H_R = 0$) for $\kappa_D = 0.1$, 1, 5, and 20 and infinity (opaque) with $N = 0.1$.

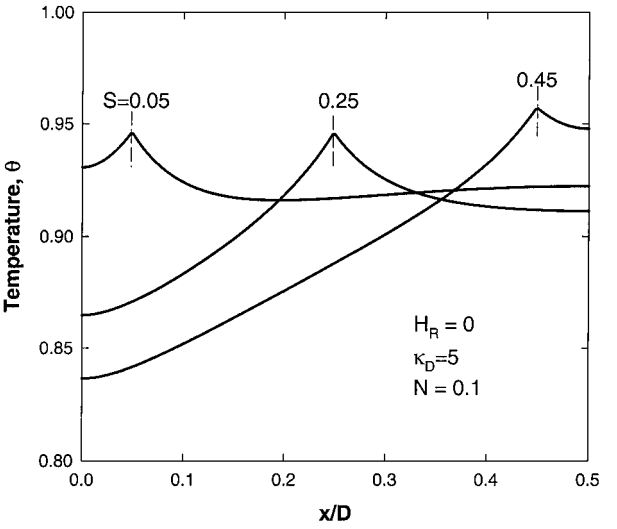

Fig. 5 Temperature distributions at the times when the interface is located at $S = 0.05$, 0.25, and 0.45 for pure radiative cooling ($H_R = 0$), $\kappa_D = 5$, and $N = 0.1$.

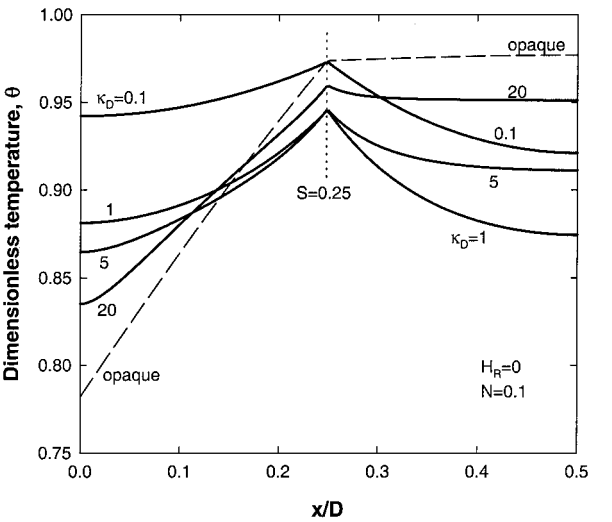

Fig. 6 Effect of optical thickness on temperature distributions at the time when the interface is at $S = 0.25$ under pure radiative cooling ($H_R = 0$) with $N = 0.1$.

κ_D on the cooling rates of a semitransparent slab in space.[29,30] Internal radiation in semitransparent materials enhances heat transfer and therefore accelerates the latent heat removal from the interface to the surroundings. This enhancement of heat transfer, however, depends on the value of the optical thickness of the material. When the optical thickness is large, reducing κ_D increases the effective emissivity of the material and thus enhances heat transfer. When the material is optically thin, however, further reduction of the optical thickness will decrease the internal heat transfer. In the limiting case, as κ_D reaches zero the material becomes completely transparent, and no radiative heat loss is possible. Figure 3 also shows that a longer time is needed to cool the surface to the nucleation temperature for a more transparent material.

The solidification velocity as a function of internal radiative heat transfer is presented in Fig. 4, where the interface velocity is plotted against the interface location. The interface velocities all start at 0.5 when the solidification is initiated, a value dictated by the preset nucleation temperature. The solidification process cannot stay at this high interface velocity because of a limited heat transfer rate. The latent heat released at the interface will heat the solidified solid as well as the nearby undercooled melt to reduce the solidification driving force and thus the interface velocity. This fast decrease in the interface velocity and rapid increase in the solidification temperature is a unique feature of nonequilibrium solidification of an undercooled melt and is often referred to as the recalescence process. For an opaque material the recalescence is followed by a quasi-equilibrium solidification process with the interface velocity decreasing slowly.[31] If the optical thickness of the material is small enough, e.g., $\kappa_D = 0.1$, 1, or 5, the interface velocity is accelerated again at the end of the recalescence before it reaches a maximum. This trend of the interface velocity variation in the beginning can be explained by the temperature distribution. During the cooling of the single-phase melt, the temperature distribution across the slab depends on the optical thickness; the smaller the optical thickness, the more uniform the temperature.[30] Therefore, for a smaller optical thickness the bulk melt is at a larger degree of undercooling when the solidification begins at the surface. After a sharp early decrease the interface velocity for a smaller optical thickness tends to increase because the interface temperature is lowered by the cold melt. For an optically thick material, however, there is a large temperature gradient near the boundary, and the interface temperature tends to increase because of the heat transfer from the melt. Figure 4 also shows that the interface velocities for $\kappa_D = 1$, 5, and 20 are higher than that for the opaque material, except in the very early stage of the solidification process. A higher interface velocity resulted from the more efficient removal of the latent heat from the interface yields a lower interface temperature. This is helpful for metastable phase formation because a higher melt undercooling can be maintained during the entire course of solidification.[25]

Figure 5 shows the temperature distributions across the slab at three time levels when the interface has advanced to $S = 0.05$, 0.25, and 0.45, respectively, for a semitransparent material with $\kappa_D = 5$. At each time level a peak exists at the solid/liquid interface, a typical temperature distribution of nonequilibrium solidification of an undercooled melt during recalescence. The appearance of a maximum temperature at the interface is caused by the rapid release of latent heat that heats up both the solid and liquid phases surrounding the interface. The peaked temperature distribution exists throughout the solidification process in a semitransparent material because a large melt undercooling remains during the entire solidification process caused by the continuous cooling of the melt by internal radiative heat transfer.

Because the internal radiation depends on the optical properties, the extent of melt undercooling during later stages of solidification is a function of the optical thickness as shown in Fig. 6, which presents the temperature profiles when the interface advances to $S = 0.25$ for five different values of optical thickness. As can be seen, the melt temperatures for all cases are below the equilibrium

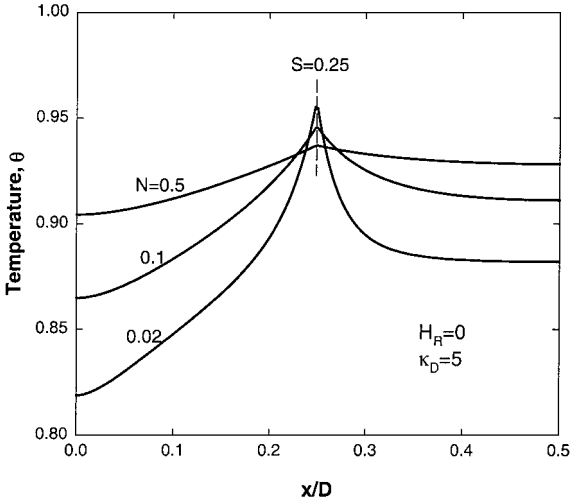

Fig. 7 Effect of the conduction-radiation parameter N on the temperature distributions at the time when the interface is at $S = 0.25$ under pure radiative cooling ($H_R = 0$) with $\kappa_D = 5$.

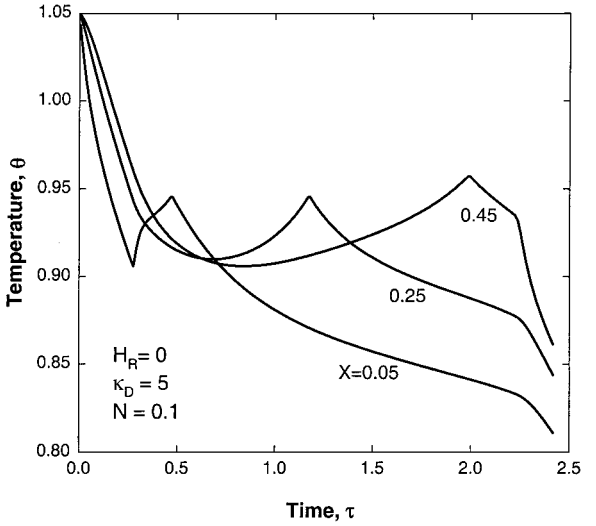

Fig. 8 Temperature histories with time at three fixed positions: $X = 0.05, 0.25$, and 0.45 under pure radiative cooling ($H_R = 0$) with $\kappa_D = 5$ and $N = 0.1$.

melting temperature with the opaque material having the smallest melt undercooling. When κ_D is greater than 1, decreasing the optical thickness leads to a decrease in the interface temperature, or an increase in the melt undercooling at the interface. This explains the variation of the interface velocity as a function of κ_D shown in Fig. 4. Figure 6 also demonstrates a significant effect of internal radiation on the overall temperature field in the material. For an opaque material energy is lost to the environment from the surface, and conduction is the only mode of internal heat transfer (in the absence of convection). As a result, a large temperature gradient is developed in the solid region, but the temperature in the melt is quite uniform. The latent heat released at the interface is transferred out of the material only through the solid region. For semitransparent materials heat is also transferred out by radiation not only from the solid region but also from the liquid region. Decreasing the optical thickness causes a more sharply distributed temperature on the melt side of the interface, mainly caused by a larger initial undercooling of the bulk melt.

The conduction-radiation parameter N is another important parameter that significantly affects the solidification process, as shown in Fig. 7. This figure illustrates the temperature distributions at $S = 0.25$ for three values of N. A small N indicates a dominating internal radiation over heat conduction. As one can see in Fig. 7, the temperature distribution for $N = 0.02$ is sharply peaked at the interface, whereas the temperature distribution for $N = 0.5$ is rather uniform. Strong heat conduction (a large N) smoothes out the temperature difference in the system and reduces the overall melt undercooling. Although a larger melt undercooling is achieved for a smaller N, a higher interface temperature results because of a low rate of heat transfer. Increasing N leads to a lower interface temperature or a higher interface melt undercooling and thus a higher interface velocity.

The recalescence phenomena can be demonstrated more clearly by examining the variation of the temperature as a function of time at fixed positions in the material. Figure 8 presents the temperature histories experienced by three points located at $X = 0.05, 0.25, 0.45$ for $\kappa_D = 5$. As can be seen, when the interface passes these points the latent heat raises all of their temperatures, resulting in a peak in the temperature histories. This is a typical feature of recalescence.

Effect of External Convective Cooling

The preceding discussion is for the case when the convective cooling is neglected on the slab surface. This is the case when processes take place in space or at an extremely high temperature difference. For many cases, however, other modes of external cooling can exist. For example, the slab may be cooled by a fluid flowing along the surface or by being placed in contact with a cold solid substrate.

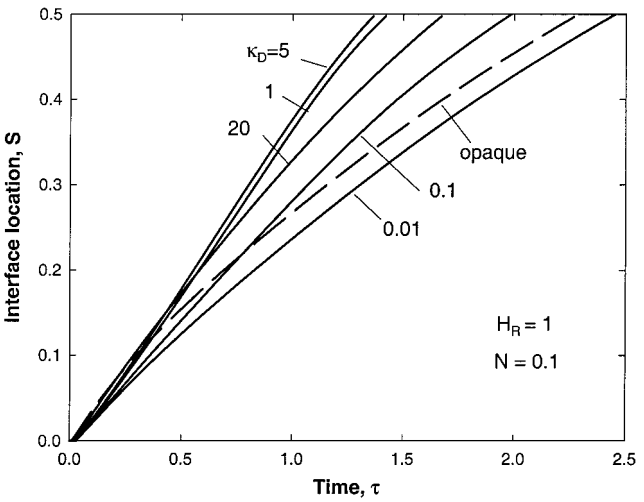

Fig. 9 Propagation of interface under combined radiative and convective cooling ($H_R = 1$) for various optical thickness with $N = 0.1$.

These external cooling modes also affect the solidification process. We are particularly interested in knowing how the external cooling alters the nonequilibrium characteristics of the process. All of those different modes of external cooling can be described by an effective convective heat transfer coefficient h_c. One can then define a convection-radiation parameter $H_R = h_c/(\sigma T_m^3)$. A high value of H_R indicates a strong external cooling effect caused by convection.

Figure 9 shows the transient solidification front locations for various values of the optical thickness when $H_R = 1$. Comparison of this figure with Fig. 3 shows that addition of surface convective cooling enhances the solidification rate, as expected, and the total solidification time is greatly shortened. For example, the solidification time is reduced from 3.9 to about 2.3 for the opaque material and from 2.4 to 1.4 for $\kappa_D = 1$. Because of the strong convective cooling on the surface, the time needed for melt at the surface to cool down to the nucleation temperature is about the same for all cases. At the early stage of the solidification, the effect of internal radiative heat transfer is relatively small. During this period, heat conduction is the dominant internal heat transfer mode because of the steep temperature gradient near the boundary. When the solidified layer becomes thicker, the effect of convective cooling reduces, and the role of internal radiation becomes more important to heat transfer around the interface. As a result, in the later stages of solidification the effect of the optical thickness on solidification characteristics

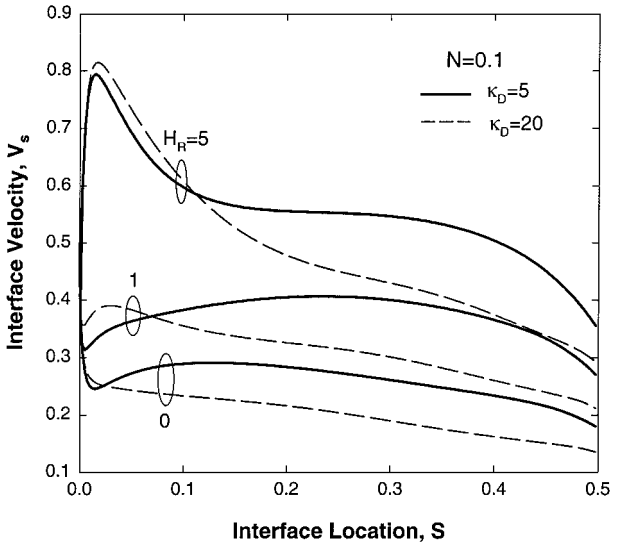

Fig. 10 Effect of the external convective cooling on the interface velocity for $\kappa_D = 5$ and 20 with $N = 0.1$.

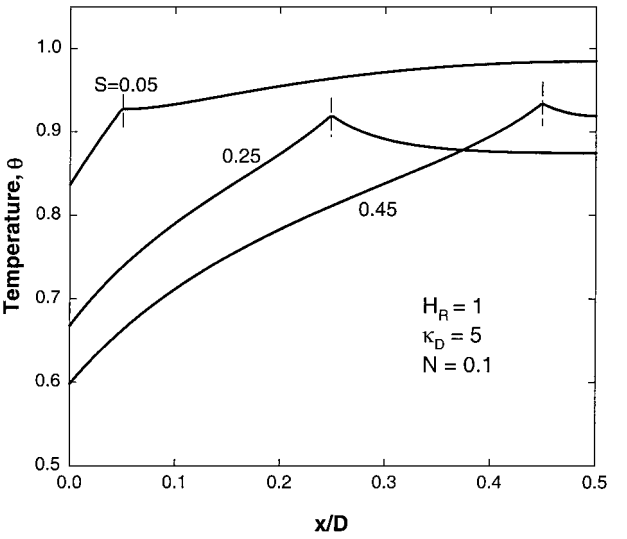

Fig. 11 Temperature distributions at the times when the interface is located at $S = 0.05$, 0.25, and 0.45 under combined radiative and convective cooling: $H_R = 1$, $\kappa_D = 5$, and $N = 0.1$.

becomes more apparent as seen in the figure. In contrast to Fig. 3, the slab with $\kappa_D = 0.1$ has a higher solidification rate than the opaque material in the later stage of solidification. This may be explained as follows. The radiative heat loss from the opaque material emanates from its surface; in the presence of external convection, the surface temperature drops rapidly and so does the radiative heat loss. On the other hand, for a semitransparent material the radiative heat loss originates from the whole volume, and the radiation also serves to enhance the internal heat transfer. This internal radiation effect exceeds the effect of surface radiation unless the material becomes optically thin, e.g., $\kappa_D = 0.01$, as shown in Fig. 9.

The effect of the external convective cooling on solidification velocities can be seen more clearly in Fig. 10, which shows the interface velocities as a function of the interface locations for three values of H_R. The solid curves are for $\kappa_D = 5$, and the dashed ones are for $\kappa_D = 20$. It is clearly seen in Fig. 10 that the external convective cooling increases the interface velocity. When H_R is increased from 0 to 5, the average solidification velocities increase by almost threefold. In addition, when H_R is sufficiently large (e.g., $H_R = 5$) the rate of heat transfer from the materials is so fast that a large melt undercooling remains at the earlier stages of solidification, and the recalescence process is thus eliminated. During this time period, the solidification rate, unlike those for $H_R = 0$ and 1, experiences an increase at the beginning until reaching a maximum. After that, the effect of the external cooling is reduced because of the added thermal resistance from the solidified layer. This kind of variation in the solidification velocity is typical for materials with a small value of the linear kinetics coefficient and a high rate of external heat transfer.[15]

The effect of external convective cooling on early stages of solidification can be further understood by inspecting the temperature distributions across the slab at various times, similar to those shown in Fig. 5. Figure 11 presents the temperature distributions at three time levels when $H_R = 1$. The temperature distribution does not show a peak at the interface when $S = 0.05$, but it does so in the later times. The temperature profile at $S = 0.05$ is similar to that during quasi-equilibrium solidification of an opaque material[31] because external convective cooling dominates the process. As the solidification proceeds, internal radiative heat transfer becomes increasingly important, leading to the similar peaked temperature profiles as shown in Fig. 5.

A peaked temperature distribution as just shown can indicate the possible development of so-called mushy zone solidification or the development of thermal dendrites. From the viewpoint of the interface stability dynamics,[32] such temperature profiles suggest a strong instability of the interface: a slight distortion of the interface plane will grow into a dendritelike front quickly because the melt in front of the interface is substantially undercooled. In other words, the present results strongly support the possibility of the existence of a mushy zone in a solidifying semitransparent material as proposed by Chan et al.[7] In this connection, a detailed investigation on the physical mechanisms of the mushy zone formation in a solidifying pure semitransparent material has been published recently.[33]

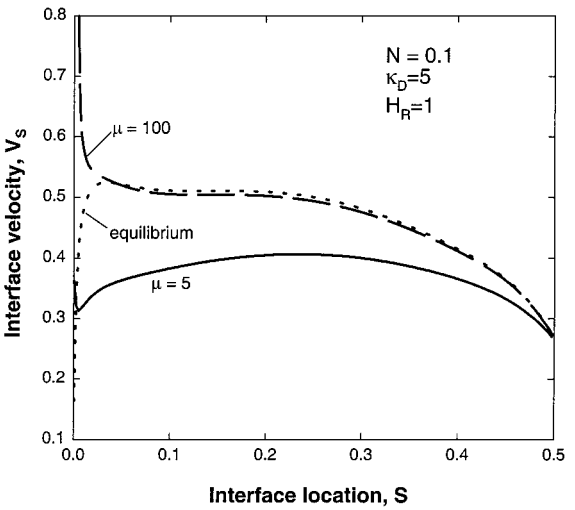

Fig. 12 Interface moving velocities for three values of kinetics coefficient, i.e., $\theta = 5$, 100, and infinity (equilibrium) under the conditions of $H_R = 1$, $\kappa_D = 5$, and $N = 0.1$.

Effect of Kinetics Coefficient

Finally, a few comments are in order about the kinetics coefficient. Throughout this paper a fixed value of $\mu = 5$ has been used for the nondimensional kinetics coefficient, which corresponds to the materials with a fairly sluggish growth kinetics, so that we can clearly illustrate the kinetics effect on solidification. As one might expect, the choice of the value of μ has a significant impact on solidification process, as shown in Fig. 12, which plots the interface velocity as a function of the interface location for three values of μ. Slower solidification kinetics (i.e., smaller μ) leads to a reduced interface velocity as in the case when $\mu = 5$. In this case the solidification is controlled by both heat transfer and solidification kinetics, as discussed earlier in this paper. When μ increases to 100, a strong kinetics effect shows only at the beginning of the solidification when

there is a large undercooling in the melt. Such a high kinetics leads to a quick reduction in the interface velocity because of recalescence, as shown in Fig. 12. The dotted line in Fig. 12 corresponds to the interface velocity obtained using an equilibrium planar interface model (e.g., Ref. 6). The equilibrium solidification can be viewed as a limiting case of the present problem with an infinitesmal initial undercooling and an infinite kinetics coefficient. In this case the solidification is solely controlled by heat transfer, and the kinetics effect disappears. It can be seen in Fig. 12 that the solidification for $\mu = 100$ approaches the equilibrium case after a short period of time. In the equilibrium process solidification begins as soon as the surface temperature drops to the equilibrium freezing temperature, and the initial interface velocity is very small. Therefore, the variation of interface velocity from the equilibrium model shows an opposite trend to the nonequilibrium cases in the early stages, as seen in Fig. 12.

The linear kinetics coefficient is a material property. For a given material the value is fixed. Whether the nonequilibrium effect is important, however, is dependent on the initial melt undercooling and the rate of heat transfer. The extent of melt undercooling is controlled by the cooling rate and nucleation kinetics of the crystalline phases, whereas the rate of heat transfer is strongly influenced by the size of the system as well as the external and internal rates of heat transfer. Generally speaking, the nonequilibrium kinetics effect becomes important only for those systems with a very small dimension but with a very fast rate of heat transfer, either external or internal or both.

In addition, even for the cases with fast solidification kinetics, solidification of a semitransparent material is an intrinsically nonequilibrium process because the bulk melt will be eventually undercooled because of internal radiation. This is different from that of an opaque material in which no bulk undercooling can exist for long when the solidification kinetics is fast.[15,31] Therefore, care must be taken in modeling the phase-change processes of semitransparent materials using an equilibrium model.

Conclusions

Results have been presented to illustrate the typical nonequilibrium solidification characteristics of a semitransparent slab under both radiative and external convective cooling conditions. Semitransparent materials have a higher solidification rate than opaque materials unless the former becomes optically thin. In the case of pure radiative cooling, a maximum rate of solidification is achieved when the optical thickness is about 1 to 5. Internal radiation leads to a large melt undercooling at the interface that may be helpful for metastable phase formation. A temperature distribution sharply peaked at the interface is found to exist throughout the solidification process; the smaller the optical thickness or the conduction parameter, the higher the temperature of the interface relative to that of the undercooled melt in front. If the external heat transfer is large enough, e.g., $H_R = 5$, the external cooling will eliminate the recalescence process, and the solidification velocity is significantly increased. Convective cooling dominates the earlier stage of solidification, and internal radiation effects become important only in the later time period.

Finally, a peaked interface temperature and a large undercooled melt in front of the moving interface strongly suggest a mushy-zone solidification for pure semitransparent materials, as proposed by the previous researchers. It is hoped that the present study sheds some light upon the physical mechanisms that control the formation of a mushy zone in a solidifying semitransparent radiating material.

Acknowledgments

The research was supported by the Computational Mechanics Research Challenge Grant sponsored by the Ohio Board of Regents. G.-X. Wang also likes to acknowledge the support of the National Science Foundation (NSF) Grant CTS-9711135 and the NSF Material Research Science Engineering Center Program at SUNY Stony Brook under Award DMR-9632570 through a subcontract to the University of Akron.

References

[1]Dorsey, N. E., *Properties of Ordinary Water Substance*, Hafner, New York, 1963, p. 404.

[2]Knight, C. A., *The Freezing of Supercooled Liquids*, Van Nostrand, Princeton, NJ, 1967, p. 125.

[3]Habib, I. S., "Solidification of Semitransparent Materials by Conduction and Radiation," *International Journal of Heat and Mass Transfer*, Vol. 14, No. 12, 1971, pp. 2161–2164.

[4]Habib, I. S., "Solidification of Semitransparent Cylindrical Medium by Conduction and Radiation," *Journal of Heat Transfer*, Vol. 95, No. 1, 1973, pp. 37–41.

[5]Goodman, T. R., "Application of Integral Methods to Transient Nonlinear Heat Transfer," *Advances in Heat Transfer,* edited by T. F. Irvine and J. P. Hartnett, Vol. 1, Academic, New York, 1964, pp. 51–122.

[6]Abrams, M., and Viskanta, R., "The Effects of Radiative Heat Transfer Upon the Melting and Solidification of Semitransparent Crystals," *Journal of Heat Transfer*, Vol. 96, No. 2, 1974, pp. 184–190.

[7]Chan, S. H., Cho, D. H., and Kocamustafaogullari, G., "Melting and Solidification with Internal Radiative Transfer—A Generalized Phase Change Model," *International Journal of Heat and Mass Transfer*, Vol. 26, No. 4, 1983, pp. 621–633.

[8]Chan, S. H., and Hsu, K. Y., "The Mushy Zone in a Phase Change Model of a Semitransparent Material with Internal Radiative Transfer," *Journal of Heat Transfer*, Vol. 110, No. 1, 1988, pp. 260–263.

[9]Diaz, L. A., and Viskanta, R., "Experiments and Analysis on the Melting of a Semitransparent Material by Radiation," *Warme- und Stoffubertragung*, Vol. 20, No. 4, 1986, pp. 311–321.

[10]Webb, B. W., and Viskanta, R., "Radiation Induced Melting with Buoyancy Effects in the Liquid," *Experimental Heat Transfer*, Vol. 1, 1987, pp. 109–126.

[11]Seki, N., Sugawara, M., and Fukusako, S., "Back-Melting of a Horizontal Cloudy Ice Layer with Radiative Heating," *Journal of Heat Transfer*, Vol. 101, No. 1, 1979, pp. 90–95.

[12]Cho, C., and Ozisik, M. N., "Effects of Radiation on the Melting of a Semi-Transparent, Semi-Infinite Medium," *Proceedings of the 6th International Heat Transfer Conference*, Vol. 3, Hemisphere, Washington, DC, 1978, pp. 373–378.

[13]Oruma, F. O., Ozisik, M. N., and Boles, M. A., "Effects of Anisotropic Scattering on Melting and Solidification of a Semi-Infinite, Semi-Transparent Medium," *International Journal of Heat and Mass Transfer*, Vol. 28, No. 2, 1985, pp. 441–449.

[14]Kim, K. S., and Yimer, B., "Thermal Radiation Heat Transfer Effects on Solidification of Finite Concentric Cylindrical Medium–Enthalpy Model and P-1 Approximation," *Numerical Heat Transfer*, Vol. 14, No. 4, 1988, pp. 483–498.

[15]Wang, G.-X., and Prasad, V., "Non-Equilibrium Phenomena in Rapid Solidification: Theoretical Treatment for Process Modeling," *Microscale Thermophysical Engineering*, Vol. 1, No. 2, 1997, pp. 143–157.

[16]Patankar, S. V., *Numerical Heat Transfer and Fluid Flow*, Hemisphere, Washington, DC, 1980, Chap. 3, pp. 25–39.

[17]Fiveland, W. A., "Discrete-Ordinates Solutions of the Radiative Transport Equation for Rectangular Enclosure," *Journal of Heat Transfer*, Vol. 106, No. 4, 1984, pp. 699–706.

[18]Voller, V. R., and Cross, M., "Accurate Solutions of Moving Boundary Problems Using the Enthalpy Method," *International Journal of Heat and Mass Transfer*, Vol. 24, No. 3, 1981, pp. 545–556.

[19]Fabbri, M., and Voller, V. R., "Numerical Solution of Planar-Front Solidification with Kinetic Undercooling," *Numerical Heat Transfer*, Pt. B, Vol. 27, No. 4, 1995, pp. 467–486.

[20]Siegel, R., and Howell, J. R., *Thermal Radiation Heat Transfer*, 3rd ed., Hemisphere, Washington, DC, 1992, Chap. 14.

[21]Modest, M. F., *Radiative Heat Transfer*, McGraw–Hill, New York, 1993, Chap. 15.

[22]Wang, G.-X., and Matthys, E. F., "Modeling of Non-equilibrium Surface Melting and Resolidification for Pure Metals and Binary Alloys," *Journal of Heat Transfer*, Vol. 118, No. 4, 1996, pp. 944–951.

[23]Siegel, R., "Transient Heat Transfer in a Semitransparent Radiating Layer with Boundary Convection and Surface Reflection," *International Journal of Heat and Mass Transfer*, Vol. 39, No. 1, 1996, pp. 69–79.

[24]Yao, C., and Chung, B. T. F., "Transient Conductive and Radiative Heat Transfer in a Rectangular Region," *Proceedings (CD) of the 33rd National Heat Transfer Conference*, NHTC99-132, edited by S. T. Thynell, D. A. Kaminski, and J. M. Ochterbeck, American Society of Mechanical Engineers, New York, 1999.

[25]Levi, C. G., and Mehrabian, R., "Heat Flow During Rapid Solidification of Undercooled Metal Droplets," *Metallurgical Transaction Part A*, Vol. 13A, No. 2, 1982, pp. 221–234.

[26]Robert, C., Denoirjean, A., Vardelle, A., Wang, G.-X., and Sampath, S., "Nucleation and Phase Selection in Plasma-Sprayed Al_2O_3: Modeling and

Experiments," *Thermal Spray: Meeting the Challenges of the 21st Century, Proceedings of the 15th International Thermal Spray Conference*, 1998, pp. 407–412.

[27]Ozisik, M. N., *Heat Conduction*, 2nd ed., Wiley-Interscience, New York, 1993, pp. 405–408.

[28]Aziz, M. J., and Boettinger, W. J., "On the Transition from Short-Range Diffusion-Limited to Collision-Limited Growth in Alloy Solidification," *Acta Metallurgica et Materialia*, Vol. 42, No. 2, 1994, pp. 527–537.

[29]Siegel, R., "Finite Difference Solution for Transient Cooling of a Radiating-Conducting Semitransparent Layer," *Journal of Thermophysics and Heat Transfer*, Vol. 6, No. 1, 1992, pp. 77–83.

[30]Yao, C., and Chung, B. T. F., "Transient Heat Transfer in a Scattering-Radiating-Conducting Layer," *Journal of Thermophysics and Heat Transfer*, Vol. 13, No. 1, 1999, pp. 18–24.

[31]Wang, G.-X., and Matthys, E. F., "Modeling of Heat Transfer and Solidification During Splat Cooling: Effect of Splat Thickness and Splat/Substrate Thermal Contact," *International Journal of Rapid Solidification*, Vol. 6, No. 2, 1991, pp. 141–174.

[32]Mullins, W. W., and Sekerka, R. F., "Stability of a Planar Interface During Solidification of a Dilute Binary Alloy," *Journal of Applied Physics*, Vol. 35, No. 2, 1964, pp. 444–451.

[33]Wang, G.-X., Yao, C., and Chung, B. T. F., "On Physical Mechanisms of Mushy Zone Formation in Solidification of Pure Semitransparent Materials," *Proceedings of ASME Heat Transfer Division—1999*, HTD-Vol. 364-2, American Society of Mechanical Engineers, New York, 1999, pp. 281–288.